AIP Applied Physics Letters

Structurally dictated anisotropic "designer surface plasmons"

Helen J. Rance, Ian R. Hooper, Alastair P. Hibbins, and J. Roy Sambles

Citation: Appl. Phys. Lett. **99**, 181107 (2011); doi: 10.1063/1.3655170
View online: http://dx.doi.org/10.1063/1.3655170
View Table of Contents: http://apl.aip.org/resource/1/APPLAB/v99/i18
Published by the American Institute of Physics.

Structurally dictated anisotropic "designer surface plasmons"

Helen J. Rance,[a)] Ian R. Hooper, Alastair P. Hibbins, and J. Roy Sambles
Electromagnetic Materials Group, Department of Physics and Astronomy, University of Exeter, Exeter, EX4 4QL, United Kingdom

(Received 19 July 2011; accepted 30 September 2011; published online 1 November 2011)

The concept of pseudo-plasmonic surfaces at microwave frequencies is extended to include structures with a high degree of surface anisotropy. The experimental sample is fabricated by patterning a metal with a rectangular array of rectangular holes and is found to support structurally dictated surface plasmon-like modes; the anisotropic dispersion of which results from an ellipsoid of limiting frequencies. By exploiting the anisotropy of the unit cell, the family of higher order surface waves associated with the quantization of the electromagnetic fields within the holes is also explored. © *2011 American Institute of Physics*. [doi:10.1063/1.3655170]

It is intrinsically difficult to induce an anisotropic response from planar metal surfaces. However, the concept of strongly bound pseudo-plasmonic or "designer" surface waves, introduced by Pendry *et al.*[1] in 2004, and the wealth of subsequent studies confirming their existence,[2–11] suggest one might be able to select specifically designed anisotropic electromagnetic properties, simply by choosing the desired symmetry of the structure.

Here, we characterize structurally dictated "designer" surface waves on a near perfectly conducting metal surface pierced by a rectangular array of close-packed, deep rectangular holes. In this arrangement, the fundamental resonance of the structure in orthogonal directions, and therefore, the frequency to which the dispersion of the surface wave is limited, is substantially different. This is in stark contrast to the optical study of Feng *et al.*[12] where anisotropy is associated primarily with diffraction (i.e., periodicity of the rectangular lattice) that strongly perturbs the dispersion of the surface mode without any variation of the limiting frequencies.

For a rectangular shaped hole of side lengths $a\underline{\hat{y}}$ and $b\underline{\hat{x}}$, there are *two* distinct waveguide cut off frequencies given by Eq. (1),

$$\nu_a = \frac{c}{2a\sqrt{\varepsilon_h \mu_h}} \text{ and } \nu_b = \frac{c}{2b\sqrt{\varepsilon_h \mu_h}}, \tag{1}$$

for electric field polarizations directed along the x- and y-axes, respectively, where c is the velocity of light in vacuum and ε_h and μ_h are, respectively, the permittivity and permeability of the material filling the holes. Furthermore, when the holes in the surface are sufficiently deep, a family of surface waves can be supported. Previous investigation into the dispersion of these higher order modes has been limited to theoretical studies on periodically structured metal surfaces formed from open groove cavities,[13] and finite depth square[14] and rectangular[15] cross-section holes. It was shown that each band is associated with a resonant mode of the cavity, resulting from the quantization of the field along its length. In this study, in addition to the anisotropy discussed above, we are also able to report the experimental observation of this family of modes. This surface asymmetry provides an additional degree of freedom in the manipulation of electromagnetic radiation using "designer" surface waves. Whilst the width of the rectangular holes in one direction (i.e., $a\underline{\hat{y}}$) dictates the resonant frequency for an incident polarization directed along the x-direction, the pitch in the orthogonal direction (i.e., $\lambda_b\underline{\hat{x}}$) dictates the onset of diffraction. Hence, we can independently control these two frequencies and tailor the geometry of the unit cell to separate these two limits, allowing for the excitation and observation of the higher order surface waves in the non-diffracting region. By employing a blade-coupling technique and using phase resolved measurements, we directly map out the dispersion of the modes in the microwave regime.

The sample (Fig. 1) is formed from an approximately 350×350 mm array of wax-filled ($\varepsilon_h = 2.25$) closed-ended rectangular brass tubes, with the inner dimensions of the

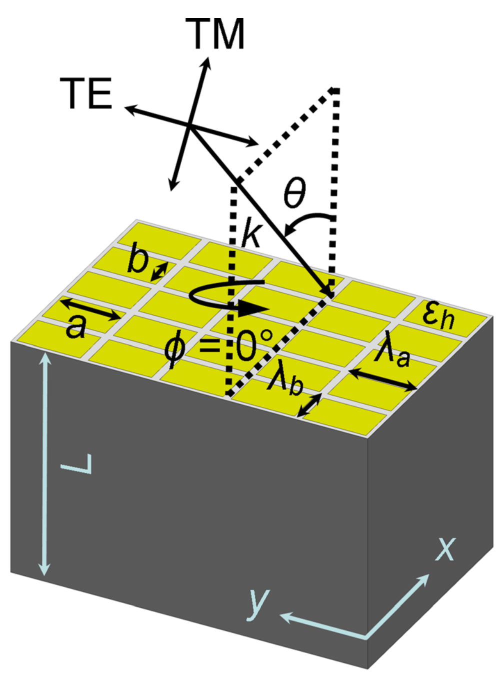

FIG. 1. (Color online) Experimental sample. The holes are of depth $L = 30$ mm and side lengths $a = 8$ mm and $b = 5$ mm. The pitches in the y- and x-directions are $\lambda_a = 9$ mm and $\lambda_b = 6$ mm, respectively. The holes are filled with dielectric (wax), $\varepsilon_h = 2.25$. Plane of incidence is shown.

[a)]Author to whom correspondence should be addressed. Electronic mail: h.j.rance@ex.ac.uk.

tubes, $a = 8$ mm and $b = 5$ mm, defining two cut-off frequencies, $\nu_a = 12.5$ GHz and $\nu_b = 20.0$ GHz, respectively. The tubes are of finite length, $L = 30$ mm; thus, the first resonant frequency of the tubes is shifted above the cut-off due to the additional quantization (approximately odd-integer quarter-wavelengths) along the tube length in the *z*-direction, such that the modified limit frequencies become $\nu'_a = 12.6$ GHz and $\nu'_b = 20.4$ GHz.

TM (Transverse Magnetic)-polarized radiation (8.0 GHz $\leq \nu \leq 30.0$ GHz) emitted from a microwave horn is coupled into the surface mode via diffraction at a 0.5 mm parallel-sided aperture formed between the sample and an aluminium blade, which lies along either the *y*- or *x*-axis. Using a second aperture placed at a distance L_1 along the surface from the first, the surface mode is coupled back into free-propagating radiation, which is then collected and detected via a second microwave horn antenna. A vector network analyser (VNA) is used to record the phase of the signal propagating across the sample. A second set of data is then taken for a larger distance L_2 for the $\phi = 0°$ orientation (i.e., the incident plane contains the vector along the short axis of the tubes). By subtracting the phase shifts of these two signals and taking the difference in propagation length $(L_2 - L_1)$ into account, the phase shift associated *only* with the mode propagation across $(L_2 - L_1)$ is extracted (with the phase shifts associated with the coupling in and out mechanisms removed). From this, the dispersion of each individual surface mode is obtained. When recording the azimuthal dependence of the fundamental surface mode, this correction is not required since its position with respect to the light line is well known. The signal can therefore be compared to that from a flat metal sheet.

Initially, TM-polarized radiation impinges on the sample surface with the incident plane containing the vector along the short axis of the tubes b ($\phi = 0°$). In this arrangement, we can readily experimentally measure the family of surface modes associated with ν_a, in the non-diffracting region since the onset of diffraction occurs at 25.0 GHz, significantly above the corresponding resonant frequency of $\nu'_a = 12.6$ GHz of the holes. Figure 2 shows the measured dispersion (circles), together with the predictions from a finite element method model (crosses) for the surface modes associated with $\phi = 0°$; they show excellent agreement. The first-order surface mode asymptotically approaches the fundamental resonance (ν'_a), and we also observe six further higher order modes in the non-diffracting region. Each surface mode in this series is associated with additional quantization of the fundamental waveguide mode (TE_{10}) (inset Fig. 2(b)) in the *z*-direction, and each of these resonances define an upper limit frequency for the respective bound surface modes. Though their surface wave character is clearly apparent from their dispersion, it is also evident in their modelled field distributions. Fig. 2(a), i-iii illustrate the time-averaged electric field strength of the fundamental, second, and third order surface modes, respectively, with the instantaneous electric field vector distribution superimposed. At the surface, regions of strong field (light regions) are clearly located directly above the metal, whilst the electric-field-line loops are highly reminiscent of surface plasmon fields on metals in the visible regime.[16] The group velocity of each mode diminishes rapidly with increasing wavevector, tending to zero as it asymptotically approaches its limiting frequency. For the majority of modes, however, the signal strength at higher wavevectors is sufficiently weak that they cannot be well characterized.

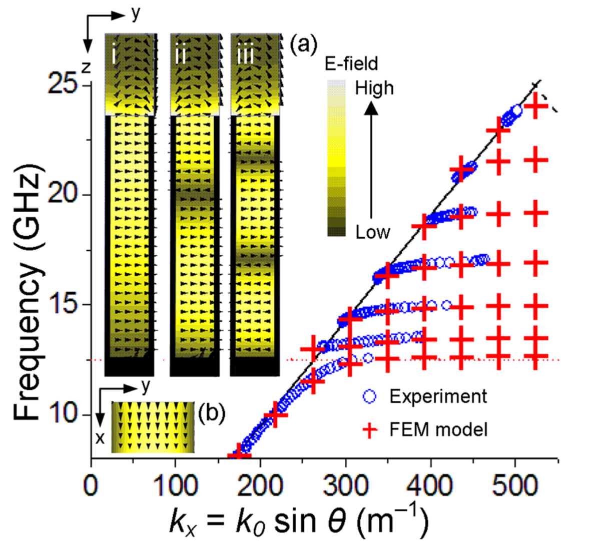

FIG. 2. (Color online) Measured dispersion (circles) together with the predictions from finite element method (Ref. 17) modelling (crosses), associated with ν_a cut-off. The dashed and dotted lines represent the first-order diffracted light lines and cut-off of the guide, respectively. Inset: Modelled time-averaged (colour map) and instantaneous (arrowheads) electric field strengths. (a) Fundamental, second, and third order surface modes. (b) TE_{10} waveguide mode. Light regions correspond to regions of highest field strength.

Consider now TM-polarized radiation impinging upon the sample, rotated to $\phi = 90°$ so that the plane of incidence contains the long axis of the unit cell. The fundamental resonance of the hole (ν_b) is increased such that the first order surface mode now approaches its limiting frequency (ν'_b) *above* the diffraction edge (Fig. 3). It does so while displaying rather limited dispersion, closely following the light line. At around 16.0 GHz in the measured data, the dispersion of the surface mode is slightly perturbed away from the light

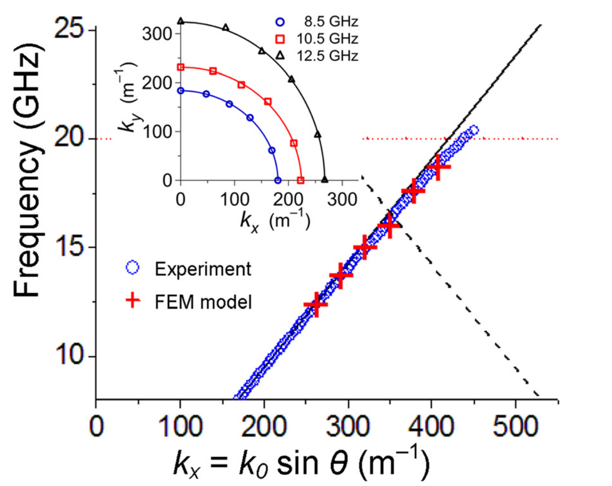

FIG. 3. (Color online) Experimentally measured dispersion (circles) together with the predictions from finite element method (Ref. 17) modelling (crosses), associated with ν_b cut-off. The dashed and dotted lines represent the first-order diffracted light lines and cut-off of the guide, respectively. Inset: Dispersion contours for selected frequencies for the fundamental mode. The experimental data (points) increases from 8.5 GHz on the inner contour (circles), which is almost circular, to 12.5 GHz on the outer contour (triangles), which is an ellipse.

line as it approaches the Brillouin zone boundary. However, since the width of the mode and the small band gap are comparable in magnitude, the expected discontinuity in the data is not observed. Recording the azimuthal dependence of the dispersion of the fundamental surface mode allows one to generate the contours that describe the surface wave dispersion (inset Fig. 3). For the lowest frequency (8.5 GHz), the contour (circles and corresponding line fit) is almost circular while at the upper frequency (12.5 GHz) an ellipse (triangles) clearly demonstrates the expected anisotropic response.

Using structure to control the limiting frequencies of bound surface waves allows one to create a tailored electromagnetic response with the desired surface symmetry. Here, we have characterised the strong anisotropy arising from a rectangular hole structure, where the fundamental surface mode has two distinct asymptotic frequencies in orthogonal directions. Furthermore, because we have been able to separate the onset of diffraction from the cut off frequency of the hole (a consequence of the rectangular unit cell), it has been possible to study the dispersion of the higher order surface modes defined by the higher quantization of the field along the length of the hole. The results obtained accord very well with finite element method modelling.[17]

The authors would like to thank the technicians, in particular Nick Cole, for their help with sample fabrication. The authors acknowledge the support of the EPSRC (UK).

[1]J. B. Pendry, L. Martín-Moreno, and F. J. García-Vidal, Science **305**, 847 (2004).
[2]F. J. García-Vidal, L. Martín-Moreno, and J. B. Pendry, J. Opt. A, Pure Appl. Opt. **7**, S97 (2005).
[3]A. P. Hibbins, B. R. Evans, and J. R. Sambles, Science **308**, 670 (2005).
[4]F. J. García de Abajo and J. J. Sáenz, Phys. Rev. Lett. **95**, 233901 (2005).
[5]Z. Ruan and M. Qiu, Phys. Rev. Lett. **96**, 233901 (2006).
[6]S. A. Maier and S. R. Andrews, Appl. Phys. Lett. **88**, 251120 (2006).
[7]S. A. Maier, S. R. Andrews, L. Martín-Moreno, and F. J. García-Vidal, Phys. Rev. Lett. **97**, 176805 (2006).
[8]Y.-C. Lan and R.-L. Chern, Opt. Express **14**, 11339 (2006).
[9]L. Shen, C. Xudong, and T.-J. Yang, Opt. Express **16**, 3326 (2008).
[10]C. R. Williams, S. R. Andrews, S. A. Maier, A. I. Fernández-Domínguez, L. Martín-Moreno, and F. J. García-Vidal, Nature Photon. **2**, 175 (2008).
[11]E. Hendry, A. P. Hibbins, and J. R. Sambles, Phys. Rev. B **78**, 235426 (2008).
[12]F. Feng, Z. Liu, V. Lomakin, and Y. Fainman, Appl. Phys. Lett. **96**, 041112 (2010).
[13]T. Jiang, L. Shen, X. Zhang, and L. Ran, Prog Electromagn. Res. **8**, 91 (2009).
[14]M. Qiu, Opt. Express **13**, 7583 (2005).
[15]Z. Ruan and M. Qiu, Appl. Phys. Lett. **90**, 201906 (2007).
[16]W. L. Barnes, A. Dereux, and T. W. Ebbesen, Nature **424**, 824 (2003).
[17]ANSOFT HFSS™ (Ansoft Corporation, Pittsburgh, PA).